

Rapidities of produced particles in 200-GeV/c π^+ / p / K^+ interactions on Au, Ag, and Mg

D. H. Brick^(a) and M. Widgoff
Brown University, Providence, Rhode Island 02912

P. Beilliere, P. Lutz, and J. L. Narjoux
College de France, Paris CEDEX 05, France

N. Gelfand
Fermilab, Batavia, Illinois 60510

E. D. Alyea, Jr.
Indiana University, Bloomington, Indiana 47401

M. Bloomer, J. Bober,^(b) W. Busza, B. Cole, T. A. Frank,^(c) T. A. Fuess,
L. Grodzins, E. S. Hafen, P. Haridas, D. Huang,^(d) H. Z. Huang, R. Hulsizer, V. Kistiakowsky,
R. J. Ledoux, C. Milstene,^(e) S. Noguchi,^(f) S. H. Oh,^(g) I. A. Pless, S. Steadman, T. B. Stoughton,^(h)
V. Suchorebrow,⁽ⁱ⁾ S. Tether, P. C. Trepagnier,^(j) B. F. Wadsworth, Y. Wu,^(d) and R. K. Yamamoto
*Department of Physics and the Laboratory for Nuclear Science, Massachusetts Institute of Technology,
Cambridge, Massachusetts 02139*

H. O. Cohn
Oak Ridge National Laboratory, Oak Ridge, Tennessee 37830

E. Calligarich, C. Castoldi, R. Dolfini, G. Introzzi, and S. Ratti
University of Pavia and Istituto Nazionale di Fisica Nucleare (INFN), Pavia, Italy

M. Badiak, R. DiMarco,^(k) P. F. Jacques, M. Kalelkar, and R. J. Plano
Rutgers University, New Brunswick, New Jersey 08903

P. E. Stamer
Seton Hall University, South Orange, New Jersey 07079

E. B. Brucker and E. L. Koller
Stevens Institute of Technology, Hoboken, New Jersey 07030

G. Alexander, J. Grunhaus, and A. Levy
Tel-Aviv University, Ramat-Aviv, Israel 69978

J. E. Brau, W. M. Bugg, G. T. Condo, T. Handler, H. J. Hargis, E. L. Hart,
A. Rafatian, and A. H. Rogers
University of Tennessee, Knoxville, Tennessee 37916

T. Kitagaki, S. Tanaka, H. Yuta, K. Abe, K. Hasegawa, A. Yamaguchi,
K. Tamai, Y. Hayaschino, and Y. Otani
Tohoku University, Sendai, Japan

M. Higuchi and M. Sato
Tohoku Gakuin University, Tagajyo, Miyagi, Japan

T. Ludlam,^(l) R. Steiner,^(m) and H. Taft⁽ⁿ⁾
Yale University, New Haven, Connecticut 06520
(Received 24 July 1989)

We have used the Fermilab 30-in. bubble chamber-hybrid spectrometer to study the rapidities of "produced particles" in the interactions of 200-GeV/c protons and π^+ and K^+ mesons with nuclei of gold, silver, and magnesium. The average rapidity decreases linearly with the number of projectile collisions ν_p (up to $\nu_p=5$) with no A dependence and little beam dependence. The ratio R of normalized rapidity distributions for hadron-nucleus to hadron-proton interactions shows a plateau

in the central region, and becomes much larger in the target region. However, the increase is significantly less than has been reported in previous experiments. As a function of v_p , the ratio R rises linearly in the target region, more gently in the central region, and decreases slowly in the projectile region, in all cases with no A dependence. Some discrepancies with a previous experiment are observed in the central region. Long-range rapidity correlations are observed in hadron-nucleus events, but not in hadron-proton events. For the former, it is shown that the correlations exist only for those events with multiple projectile collisions, as expected in the multichain dual parton model.

We have recently published¹ a study of multiparticle production in the interactions of 200-GeV/ c protons and π^+ and K^+ mesons with nuclei of gold, silver, and magnesium. In that paper we investigated the correlations of multiplicities and dispersions with the numbers of projectile and secondary collisions in the nucleus. In this work, based on the same experiment, we report a study of rapidities and rapidity correlations, again emphasizing the dependence on the number of projectile collisions. Previous results on the general topic of rapidities in hadron-nucleus collisions have been reviewed by Fredriksson *et al.*² and by Busza and Ledoux.³ A notable feature of our experiment is that we have three different incident beam types and three different targets, thereby providing nine reactions all analyzed in an identical manner.

The experiment was performed at Fermilab using the 30-in. bubble chamber-hybrid spectrometer system. Experimental details have been reported elsewhere;^{1,4} here we summarize only the most significant features. A tagged secondary beam of 200-GeV/ c positively charged particles was incident on the detector. The upstream spectrometer achieved beam definition using scintillator counters and proportional wire chambers (PWC's), and identified each beam particle by using three Cherenkov counters. For the data reported in this paper, the beam composition was 49% π^+ , 35% p , and 16% K^+ . The targets consisted of six thin (~ 1 mm) metal plates, two each of gold, silver, and magnesium, located inside the bubble chamber at its upstream end. The rest of the chamber was filled with liquid hydrogen and placed in a 2-T magnetic field. The downstream spectrometer used PWC's and drift chambers to track fast charged particles for accurate momentum determination.

Photographs of the chamber, which were taken for each burst of incoming beams, were scanned for events occurring in the plates and in the liquid. Precision measurements of all tracks of an event were made with a semiautomatic precision-encoding and pattern-recognition (PEPR) device, and the program GEOHYB provided the geometrical reconstruction of the event. Particular emphasis was placed on the accurate reconstruction of every track of an event, which was especially difficult because the hadron-nucleus events were far more complex than hadron-nucleon events, with multiplicities as high as 97 prongs. Physicists examined all events on the scan table to check the geometrical reconstruction, and remeasurements were made as necessary until a complete and correct reconstruction was achieved. The physicist also identified each track by its ionization whenever that was possible. This technique allowed the

identification of protons up to a momentum of 1.2 GeV/ c , and electrons up to a momentum of 140 MeV/ c . All other tracks were taken to be pions.

To obtain our data sample, we imposed the requirement of more than three charged particles in the final state, so as to compensate for different scanning biases in low-multiplicity hydrogen and plate events, and to remove elastic events. After this cut, the sample consisted of 1313 plate events and 896 hydrogen events. Table I shows the division of these events among the various beam types and targets.

For the analysis reported here, we define the rapidity in the laboratory frame as $y = \frac{1}{2} \ln[(E + P_L)/(E - P_L)]$, where E and P_L are the total laboratory energy and longitudinal momentum of the particle under consideration. (The rapidity in the hadron-nucleon center-of-mass frame is shifted by 3.0 units.) We follow the usual practice of presenting the rapidities only of "produced particles," which we define as all particles except those identified as protons from ionization. Figure 1 shows normalized rapidity distributions of produced particles separately for the π^+ and p beams, and also separated by target type. The distributions are normalized to the total number of events N for each reaction, so that the ordinate at any point represents the average multiplicity of produced particles per unit interval of rapidity. Even at the highest momenta, our resolution in rapidity is generally no worse than 0.1 units, and for the bulk of the particles the resolution is much better. Since our bin size in the figure is 0.5 units, resolution does not significantly influence the shapes.

The qualitative features of the figure can be understood by considering the effects of multiple projectile collisions. For each beam type, as the target mass A increases, the distributions shift to lower rapidities and their heights increase. As noted in our previous paper,¹ multiplicities increase linearly with the number of projectile collisions,

TABLE I. Number of events in each data sample.

Target	π^+ beam	p beam	K^+ beam
Au	230	181	97
Ag	259	255	85
Mg	80	101	25
H	326	359	211

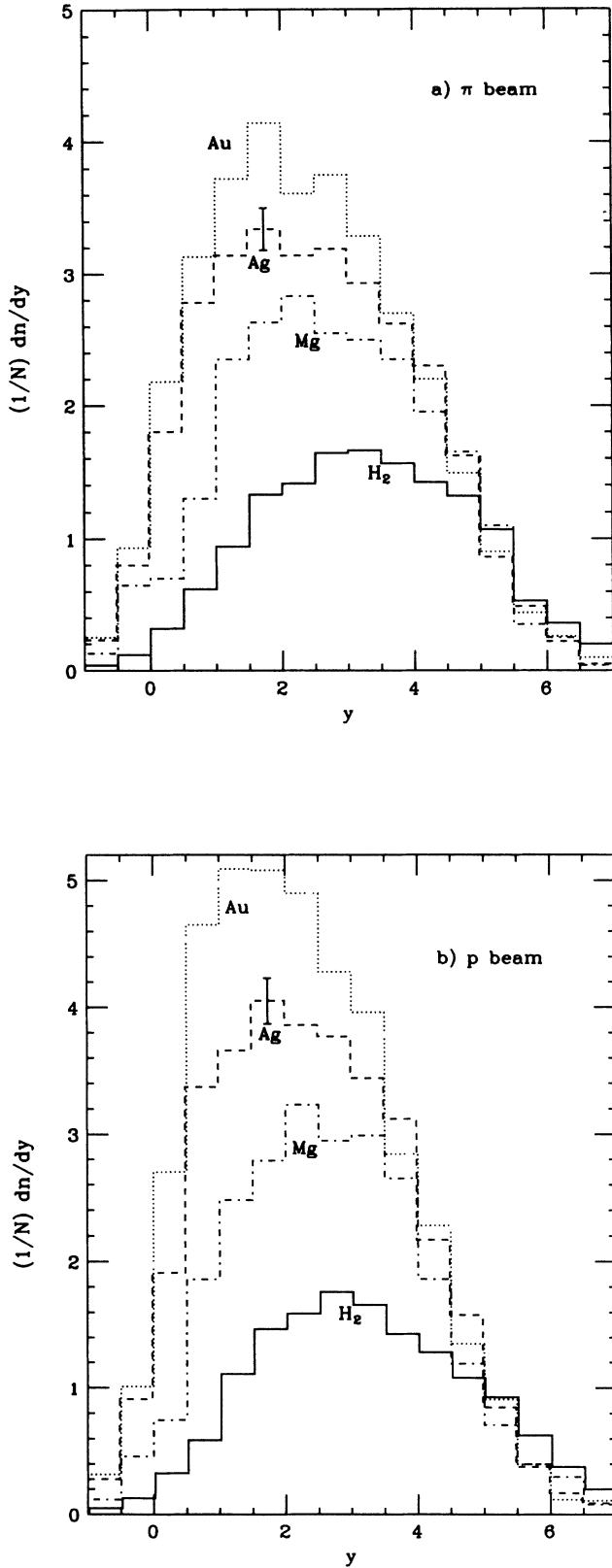


FIG. 1. Rapidity distributions of all produced particles, normalized to the total number of events in each reaction, for (a) π^+ beam and (b) proton beam. The rapidities are in the laboratory frame, and are shown separately for the three metal targets and for hydrogen.

which in turn increase with A , thereby raising the heights of the distributions. However, as the number of collisions increases, the energy of the projectile has to be shared by more particles, so that the average rapidity decreases. It may be noted that for large values of rapidity the distributions for all targets come close together and possibly even exhibit a crossover. Because of energy conservation, the amount of particle production at high rapidities is limited. A crossover is plausible since the projectile itself gradually loses energy by repeated collisions inside the nucleus. Finally, the proton beam does induce more projectile collisions than the π beam,¹ which accounts for the difference in heights of the rapidity distributions for those two beams for any given target. The distributions for the K beam are similar to those for the π beam, but with reduced statistical accuracy.

Additional information can be obtained by examining the ratio $R(y)$ of normalized rapidities for hadron-nucleus interactions to those for hadron-proton interactions: $R(y) = [(1/N)dn/dy]_{hA} / [(1/N)dn/dy]_{hp}$. Such plots have been published by DeMarzo *et al.*⁵ using streamer-chamber data on 200-GeV/c p and \bar{p} interactions with Xe and Ar, and by Bailly *et al.*⁶ using European Hybrid Spectrometer data on 360-GeV/c proton collisions on Au and Al. In Fig. 2 we show $R(y)$ for our π

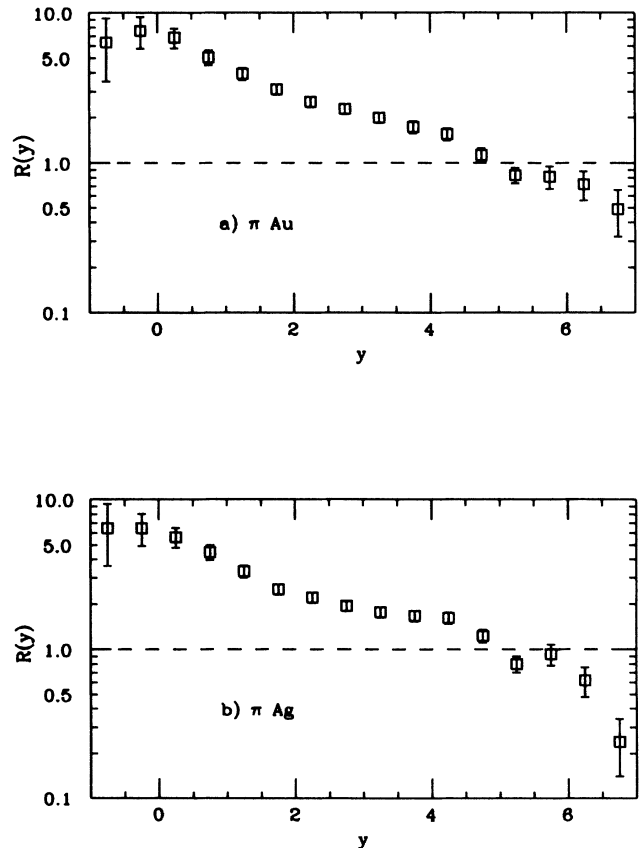


FIG. 2. Ratio of normalized rapidity distributions of all produced particles for π^+ -nucleus interactions to those for π^+ - p interactions, for (a) gold target and (b) silver target.

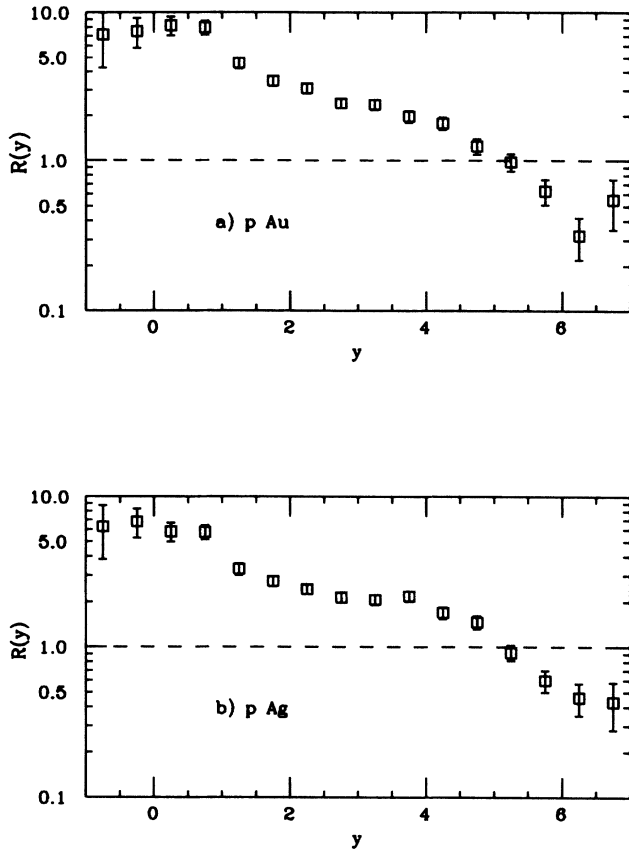


FIG. 3. Ratio of normalized rapidity distributions of all produced particles for p -nucleus interactions to those for p - p interactions, for (a) gold target and (b) silver target.

beam on Au and Ag targets, and the corresponding plots for p and K^+ beams are in Figs. 3 and 4, respectively. Our statistics are intermediate between those of Refs. 5 and 6, but we have data from meson as well as proton beams, while Refs. 5 and 6 have nucleon beams only.

In the projectile fragmentation region ($y > 5$) we observe that $R(y)$ is less than one for all combinations of beams and targets. No doubt this reflects the projectile's loss of energy in repeated collisions, as was mentioned above in the discussion of crossover in Fig. 1. In the central region ($2 < y < 4$) there is a suggestion of a plateau, with only a weak dependence on y . The value of the plateau ($R \sim 2$) is sometimes identified with the average number of wounded constituents of the beam in a number of models,⁷ such as the additive quark model. In the target-fragmentation region ($y < 1$) the ratio $R(y)$ becomes much larger, because secondary collisions of recoiling nucleons inside the nucleus induce multiplication of low-momentum particles.¹ However, it is in this target region that we observe some disagreements with the results of Ref. 5. For all our beams and targets, $R(y)$ at low rapidities does not exceed a value of about 7 or 8. DeMarzo *et al.*⁵ reported significantly higher values, especially for p -Xe data, where they found $R(y)$ exceeding 30. Proton contamination may be a pertinent factor, since they identified protons only up to 0.6 GeV/c,

whereas our identification extends up to 1.2 GeV/c. We also have some disagreement, although smaller, with Bailly *et al.*,⁶ who reported $R(y) \sim 20$ for low rapidities for 360 GeV/c p -Au collisions. However, they did not select produced particles in the same way as we and Ref. 5 did, instead defining "shower" particles as all those with bubble densities less than 1.3 times minimum ionizing.

To eliminate any complications due to proton contamination, we show the rapidity ratios $R_-(y)$ of negative particles in Figs. 5 and 6 for π and p beams, respectively. We observe that they are very similar to $R(y)$, which suggests to us that our data for $R(y)$ are not significantly affected by protons. We do find that there are many protons in the momentum range 0.6–1.2 GeV/c, so that we would expect an experiment like Ref. 5 to exhibit higher values of $R(y)$ at low y than we do. On the other hand, Ref. 5 found that their distribution of $R_-(y)$ was also similar to their $R(y)$, which argues against protons as the explanation for their high $R(y)$.

In our previous paper¹ we found that the most important quantity for describing the interaction between a hadron beam (h) and a target nucleus (A) is ν_p , the number of projectile collisions that occurred inside the nucleus. For a given reaction (hA) the average value of this quantity is⁸ $\langle \nu_p \rangle = A(\sigma_{hp}/\sigma_{hA})$, where σ_{hp} and σ_{hA} are

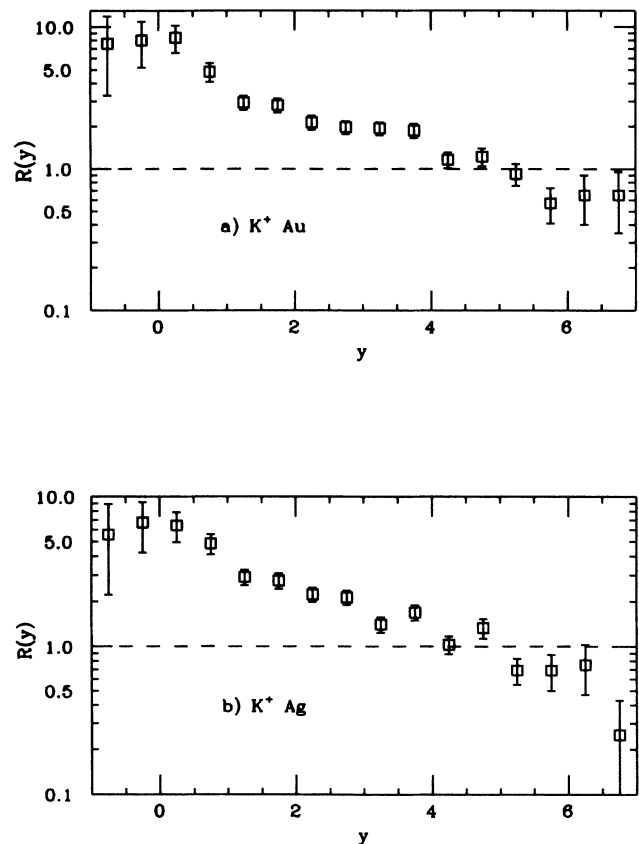


FIG. 4. Ratio of normalized rapidity distributions of all produced particles for K^+ -nucleus interactions to those for K^+ - p interactions, for (a) gold target and (b) silver target.

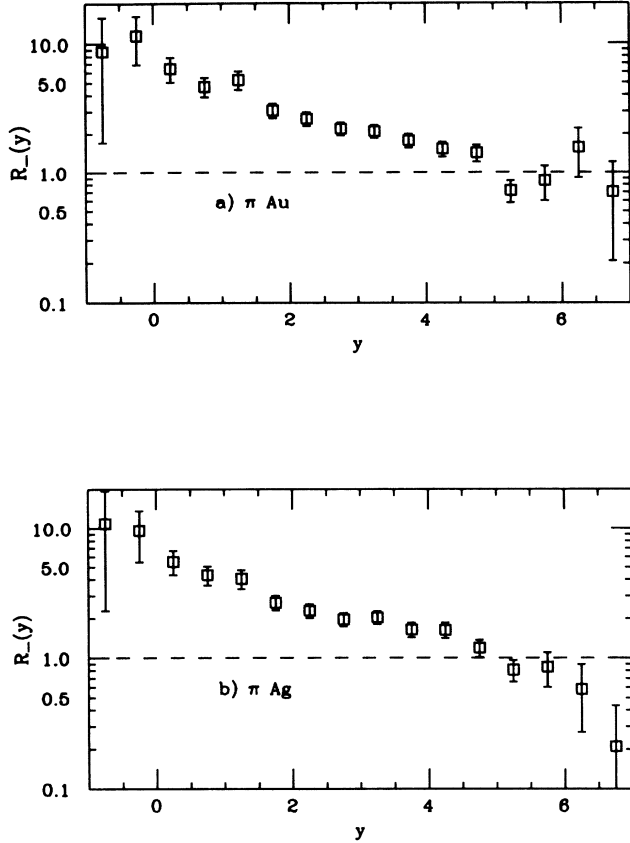


FIG. 5. Ratio of normalized rapidity distributions of negative produced particles for π^+ -nucleus interactions to those for π^+ - p interactions, for (a) gold target and (b) silver target.

the inelastic cross sections for hadron-proton and hadron-nucleus collisions, respectively. To obtain an event-by-event estimate, we define⁹ $v_p(n_p) = C_{hA} \sqrt{n_p}$, where n_p is the number of “grey” protons (i.e., identified protons of momentum greater than 0.3 GeV/c) in the event. The proportionality constant C_{hA} is chosen so that the average value of $v_p(n_p)$ over all events of a given reaction (hA) will be equal to $\langle v_p \rangle$ for that reaction as given by the formula above. With this definition, we previously found¹ that produced-particle multiplicities depend only on $v_p(n_p)$ and not on beam or target type separately.

In Fig. 7 we show the average rapidity of produced particles as a function of v_p . In Fig. 1 we had noted that the rapidity distributions shifted to lower values of y as the target mass increased. We now see directly in Fig. 7 that the decrease in rapidity is due to increasing numbers of projectile collisions; the energy has to be shared by more and more particles as v_p increases. Indeed, in Fig. 7 we observe that when plotted as a function of v_p , the average rapidity has no target dependence. For all three beams the decrease is linear for low values of v_p , but eventually exhibits a leveling off. For the π and p beams, the leveling occurs at about $v_p = 5$, but for the K beam it seems to set in earlier. In the linear region, the slopes are

-0.27 ± 0.02 , -0.21 ± 0.02 , and -0.30 ± 0.03 for the π , p , and K beams, respectively.

DeMarzo *et al.*¹⁰ have found it instructive to divide the rapidity interval into three regions, and in each one to examine R as a function of v_p , where R is the ratio of normalized rapidity distributions for hadron-nucleus to hadron-proton collisions. For ease of comparison with Ref. 10, we have used the same definitions of the three rapidity regions: (i) the target-fragmentation region, $y < 2.0$; (ii) the central production region, $2.4 < y < 3.6$; and (iii) the projectile-fragmentation region, $y > 5.0$. (DeMarzo *et al.* deliberately left gaps between the regions so as to eliminate transition effects). From Figs. 2–4 it is clear that these definitions are suitable for our data as well. We have fewer events than Ref. 10, but we do have meson as well as proton beams, whereas Ref. 10 reported proton-beam data only.

Figure 8 shows R as a function of v_p in the target-fragmentation region. In agreement with Ref. 10 we observe a linear rise with no target dependence. There is not much beam dependence either; for the π , p , and K beams, respectively, the slopes are 1.7 ± 0.1 , 1.3 ± 0.1 , and 1.6 ± 0.2 .

Figure 9 is a similar plot for the central region. Here we observe a much gentler increase of R with v_p . This general behavior is expected in a number of models⁷ and

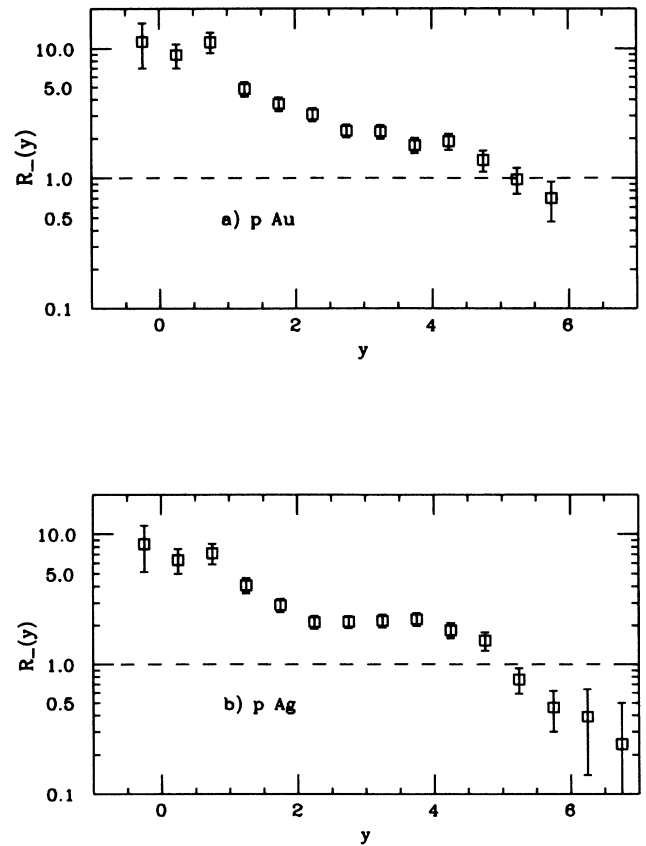


FIG. 6. Ratio of normalized rapidity distributions of negative produced particles for p -nucleus interactions to those for p - p interactions, for (a) gold target and (b) silver target.

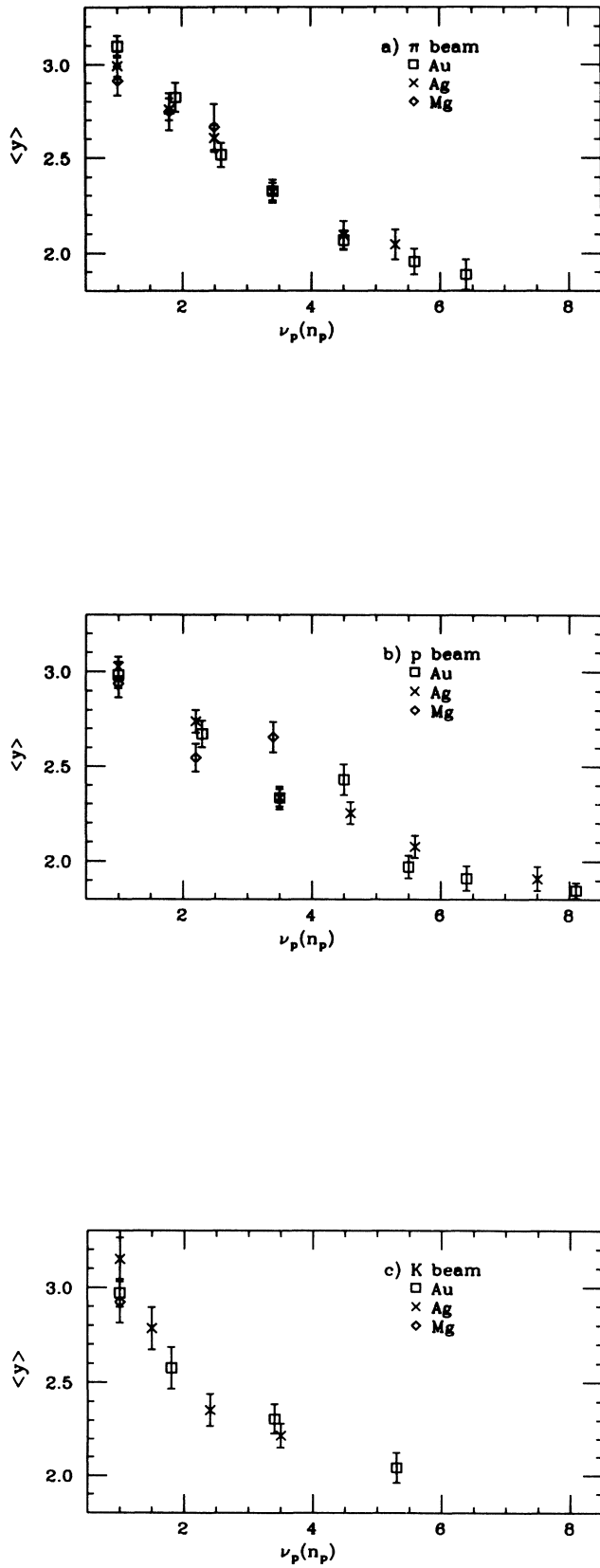


FIG. 7. Average rapidity of all produced particles as a function of the number of projectile collisions, for (a) π^+ beam, (b) p beam, and (c) K^+ beam. The number of collisions was estimated event by event from the grey-proton multiplicity.

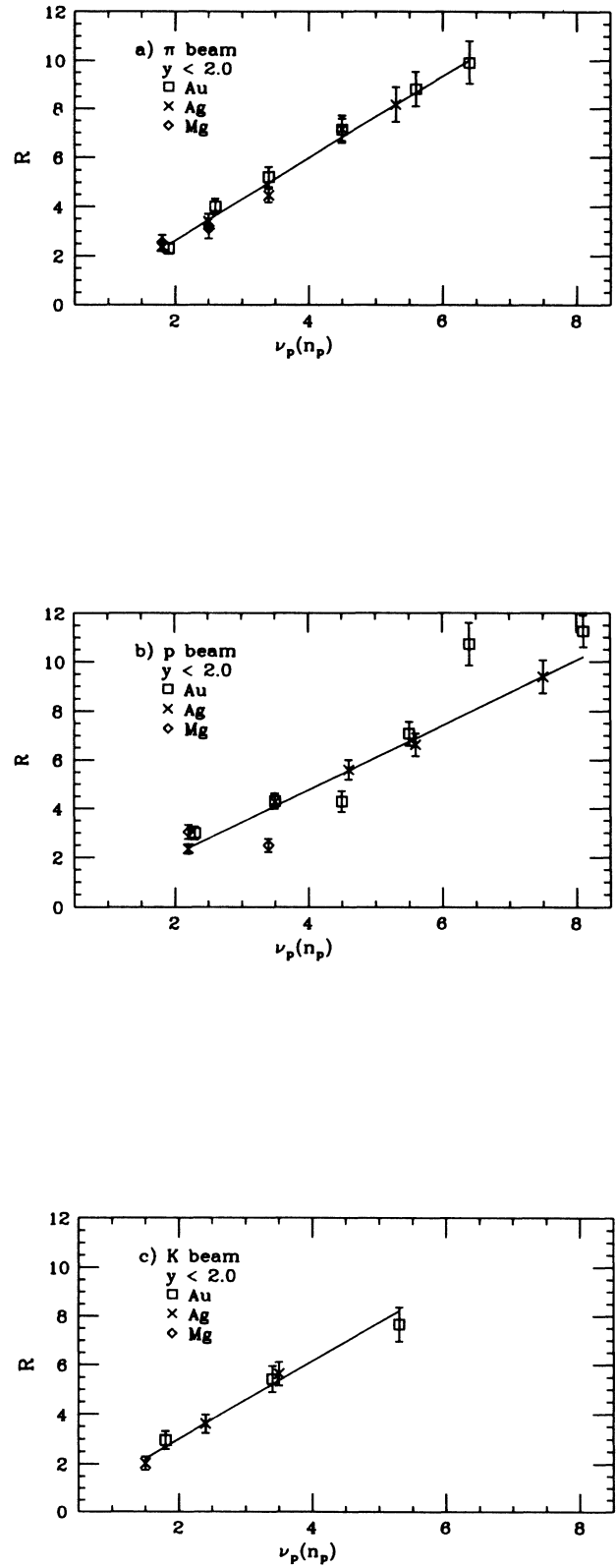


FIG. 8. Ratio of normalized rapidity distributions in the target-fragmentation region for hadron-nucleus to hadron-proton interactions, for (a) π^+ beam, (b) p beam, and (c) K^+ beam, shown as a function of the number of projectile collisions. The lines represent linear fits to the data, and the slopes are given in the text.

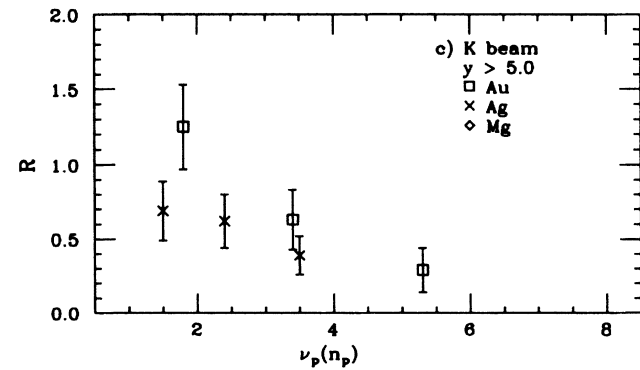
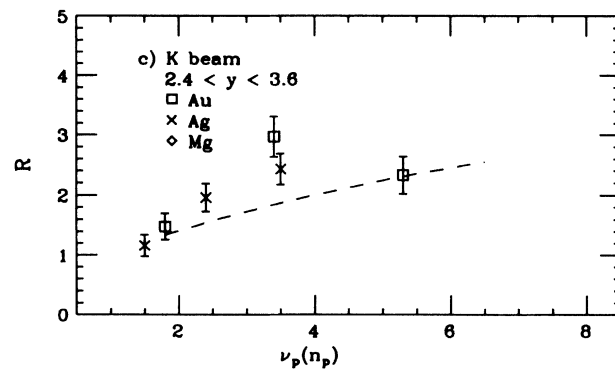
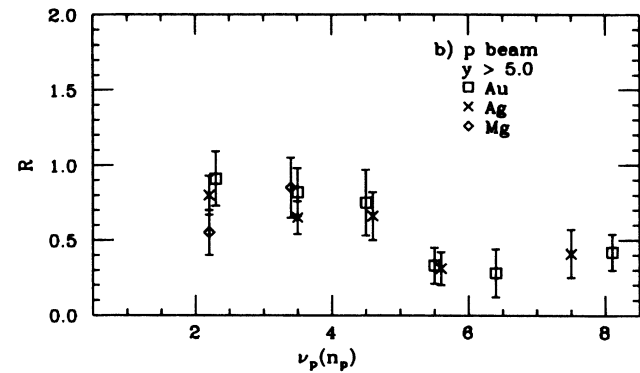
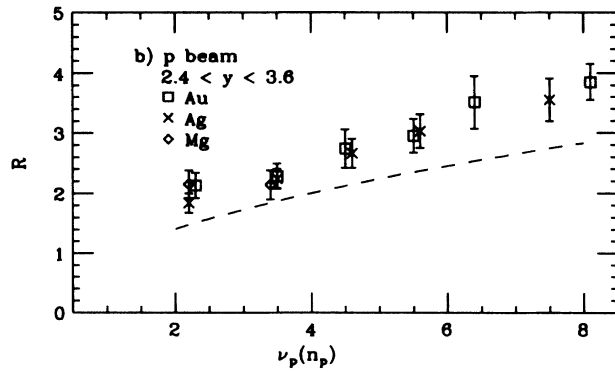
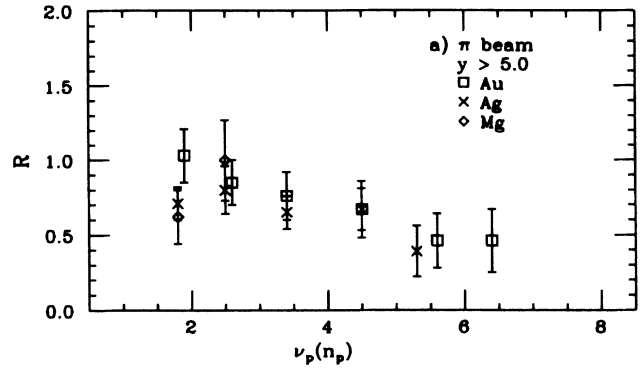
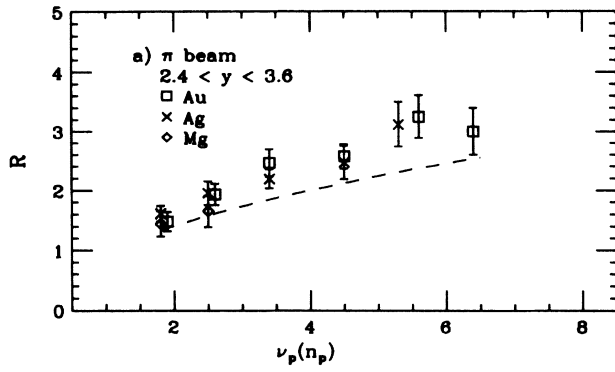


FIG. 9. Ratio of normalized rapidity distributions in the central region for hadron-nucleus to hadron-proton interactions, for (a) π^+ beam, (b) p beam, and (c) K^+ beam, shown as a function of the number of projectile collisions. The dashed lines represent the curve $R = \sqrt{\nu_p}$, which was found to describe the data of Ref. 10.

FIG. 10. Ratio of normalized rapidity distributions in the projectile fragmentation region for hadron-nucleus to hadron-proton interactions, for (a) π^+ beam, (b) p beam, and (c) K^+ beam, shown as a function of the number of projectile collisions.

is qualitatively in agreement with Ref. 10. However, the detailed behavior shows some discrepancies with Ref. 10. Kerman, Matsui, and Svetitsky¹¹ have shown that a color flux-tube model predicts $R = \sqrt{\nu_p}$ (at least for proton-beam events) and that this form gives a good description of the data of Ref. 10. Li and Young¹² have shown that their partition-temperature model also fits the same data.

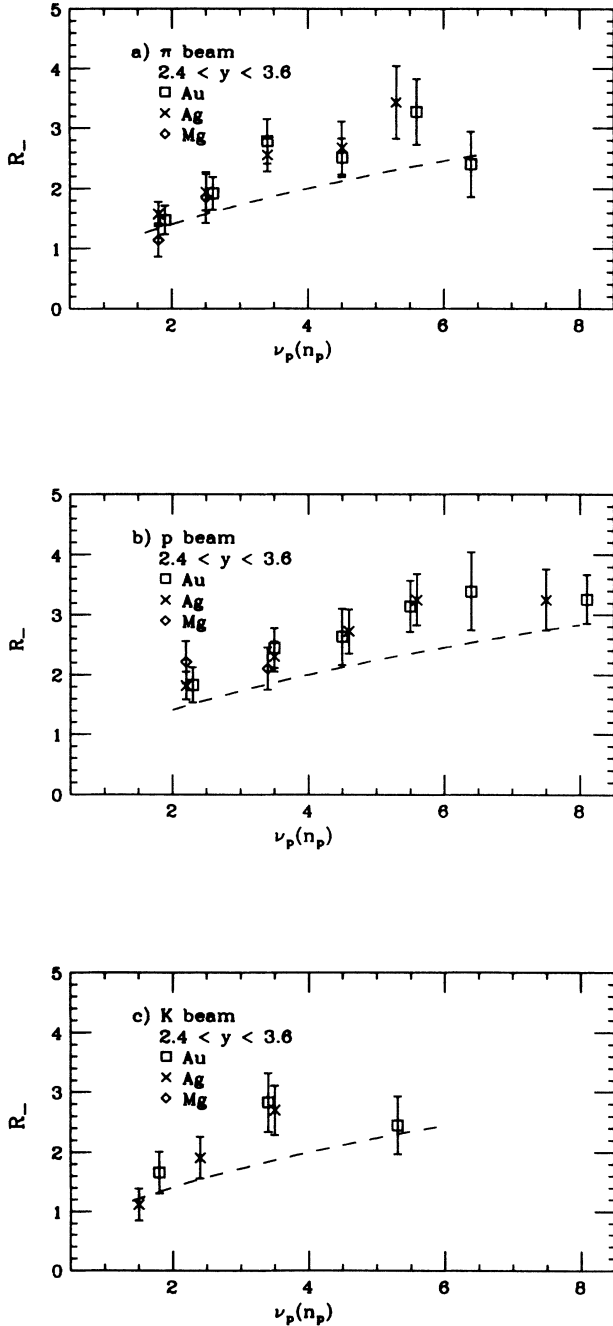


FIG. 11. Ratio of normalized rapidity distributions of negative produced particles in the central region for hadron-nucleus to hadron-proton interactions, for (a) π^+ beam, (b) p beam, and (c) K^+ beam, shown as a function of the number of projectile collisions. The dashed lines represent the curve $R = \sqrt{\nu_p}$.

In Fig. 9 we have included the curve $R = \sqrt{\nu_p}$ for comparison, and we see that our points consistently seem to lie above it, especially for the proton beam. This result does not depend sensitively on the exact definition of the central region.

Our statistical errors are greatest in the projectile-fragmentation region, for which Fig. 10 shows R as a function of ν_p . Once again there is no evidence for target dependence, and the data for each beam type exhibit a slow decline which probably reflects the projectile's loss of energy as more collisions occur, which has been discussed earlier in this paper.

We have noted previously that we can identify protons up to a momentum of 1.2 GeV/c. To avoid the problem of proton contamination in the central region, we have calculated R_- , the ratio of normalized rapidity distributions of negative particles for hadron-nucleus to hadron-proton events. We show this ratio in the central region in Fig. 11, which is analogous to Fig. 9. For convenience we have reproduced the curve $\sqrt{\nu_p}$ in the figure. The data are quite similar to Fig. 9, and suggest that proton contamination is not a significant influence on the trend.

Hadron-proton interactions at moderate energies have long been known to exhibit short-range rapidity correlations. However, at very high energies ($\sqrt{s} = 540$ GeV) the UA5 experiment at CERN has reported¹³ long-range correlations in particle rapidities. Capella and Tran

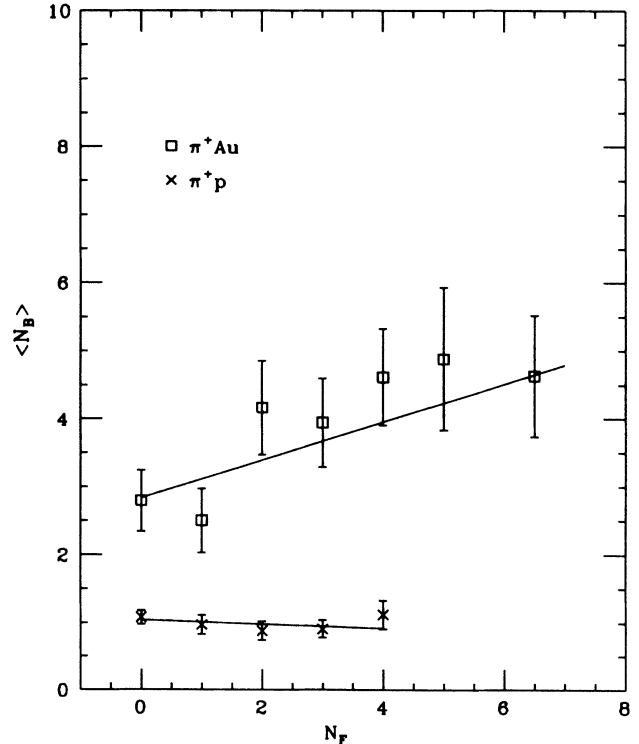


FIG. 12. Average charged multiplicity in the rapidity region (0.75, 1.75) as a function of charged multiplicity in the region (3.25, 4.25), for π^+p and π^+Au interactions. The lines represent linear fits to the data, and their slopes (see Table II) are a measure of long-range rapidity correlations.

TABLE II. Slope parameter b for long-range correlations, where $\langle N_B \rangle = a + bN_F$.

Target	π^+ beam	p beam
H	-0.03 ± 0.04	-0.02 ± 0.05
Mg	0.02 ± 0.28	0.25 ± 0.21
Ag	0.40 ± 0.09	0.39 ± 0.09
Au	0.40 ± 0.12	0.55 ± 0.15
Events with $n_p = 0$	-0.04 ± 0.09	-0.12 ± 0.09
Events with $n_p > 0$	0.40 ± 0.09	0.55 ± 0.10

Thanh Van¹⁴ have noted that multiple inelastic scattering may be the mechanism producing these long-range correlations, in which case hadron-nucleus interactions should exhibit the phenomenon even at more moderate energies. Using the multichain dual parton model, Capella and Tran Thanh Van have determined that it is essential to select rapidity intervals judiciously in order to observe long-range correlations. For 200 GeV/c proton-nucleus collisions, they have predicted correlations between multiplicities in a "forward" region defined by $y = 3.25-4.25$, and a "backward" region defined by $y = 0.75-1.75$. Derado *et al.*¹⁵ have tested this prediction using the streamer-chamber data of Ref. 10. They have performed fits to their data of the form $\langle N_B \rangle = a + bN_F$, where N_F is the charged multiplicity in the forward region as defined above, and $\langle N_B \rangle$ is the corresponding average charged multiplicity in the backward region. For the slope b they obtained -0.01 ± 0.01 for p - p data, and 0.41 ± 0.04 for p -Xe data, thereby confirming the prediction of long-range correlations in hadron-nucleus interactions.

We have selected the same rapidity intervals for our in-

vestigation of possible long-range correlations. In Fig. 12 we show the correlation between $\langle N_B \rangle$ and N_F for our π^+p and π^+Au data. As expected, the hydrogen data show no evidence for any correlation, and the linear fit produces a slope of -0.03 ± 0.04 . By contrast, the gold events do exhibit clear correlation, with a slope of 0.40 ± 0.12 . Table II gives the slopes for all such fits for our π^+ and proton-beam interactions on hydrogen and on the three metal plates. For both beams, we find no correlation for hydrogen and significant correlation for gold and silver. (The statistics do not allow a meaningful result for the magnesium target or for the K beam.)

We have attempted an additional test of Capella and Tran Thanh Van's suggestion that long-range correlations are a consequence of multiple inelastic scattering. For each beam we have combined the data for all three metal plate targets, and then divided the events into two categories: those with and without grey protons. Events with $n_p = 0$ can be expected¹ to be a fairly pure sample of events in which only one projectile collision occurred, while events with $n_p > 0$ should mostly consist of events with multiple collisions. In Table II we give the slope parameters for these samples. For both beams we find that the events with $n_p = 0$ have slopes consistent with zero, while the events with $n_p > 0$ have clearly significant nonzero slopes. Therefore our data do corroborate the hypothesis of Capella and Tran Thanh Van.

We are grateful to the scanning and measuring staffs at our respective institutions for their painstaking work. We also thank Fermilab and the 30-in. bubble chamber crew for making the experiment possible. This research was supported in part by funds provided by the U.S. Department of Energy, the National Science Foundation, the U.S.-Israel Binational Science Foundation, the Italian Istituto Nazionale di Fisica Nucleare, and by the Japan Society for the Promotion of Science.

^(a)Present address: P.O. Box 63, A.P.O. San Francisco, CA 96555.
^(b)Present address: Center for Naval Analysis, 200 N. Beauregard Street, Alexandria, VA 22311.
^(c)Present address: 17 East 67 Street, Apt. 3B, New York, NY.
^(d)Present address: Institute of High Energy Physics, Beijing, People's Republic of China.
^(e)Present address: Tel-Aviv University, Ramat-Aviv, Israel 69978.
^(f)Present address: Nara Women's University, Nara, Japan.
^(g)Present address: Duke University, Durham, NC 27706.
^(h)Present address: General Motors Technical Ct., Warren, MI 48090.
⁽ⁱ⁾Present address: 1801 N. Beauregard Street, Alexandria, VA 22311.
^(j)Present address: Automatix, Burlington, MA 01803.
^(k)Present address: Arete Associates, P.O. Box 16287, Arlington, VA 22215-1287.
^(l)Present address: Brookhaven National Lab., Upton, NY 11973.
^(m)Present address: Columbia University, New York, NY 10027.

⁽ⁿ⁾Deceased.

¹D. H. Brick *et al.*, Phys. Rev. D **39**, 2484 (1989).
²S. Fredriksson, G. Eilam, G. Berlad, and L. Bergstrom, Phys. Rep. **144**, 187 (1987).
³W. Busza and R. Ledoux, Annu. Rev. Nucl. Part. Sci. **38**, 119 (1988).
⁴R. DiMarco, Ph.D. thesis, Rutgers University, 1985.
⁵C. DeMarzo *et al.*, Phys. Rev. D **26**, 1019 (1982).
⁶J. L. Bailly *et al.*, Z. Phys. C **35**, 301 (1987).
⁷For a review of models, see K. Fialkowski and W. Kittel, Rep. Prog. Phys. **46**, 1283 (1983).
⁸W. Busza, Acta Phys. Pol. **B8**, 333 (1977).
⁹W. Q. Chao, M. K. Hegab, and J. Hufner, Nucl. Phys. **A395**, 482 (1983).
¹⁰C. DeMarzo *et al.*, Phys. Rev. D **29**, 2476 (1984).
¹¹A. K. Kerman, T. Matsui, and B. Svetitsky, Phys. Rev. Lett. **56**, 219 (1986).
¹²T. S. Li and K. Young, Phys. Rev. D **34**, 142 (1986).
¹³K. Alpgard *et al.*, Phys. Lett. **123B**, 361 (1983).
¹⁴A. Capella and J. Tran Thanh Van, Phys. Rev. D **29**, 2512 (1984).
¹⁵I. Derado *et al.*, Z. Phys. C **40**, 25 (1988).